Guidelines for Poisson Solvers on Irregular Domains with Dirichlet Boundary Conditions Using the Ghost Fluid Method

Yen Ting Ng [*] Han Chen [†] Chohong Min [‡] Frédéric Gibou [§]

November 4, 2008

Abstract

We consider the variable coefficient Poisson equation with Dirichlet boundary conditions on irregular domains. We present numerical evidence for the accuracy of the solution and its gradients for different treatments at the interface using the Ghost Fluid Method for Poisson problems of Gibou *et al.* [8, 6]. This paper is therefore intended as a guide for those interested in using the GFM for Poisson-type problems (and by consequence diffusion-like problems and Stefan-type problems) by providing the pros and cons of the different choices for defining the ghost values and locating the interface. We found that in order to obtain second-order-accurate gradients, both a quadratic (or higher order) extrapolation for defining the ghost values and a quadratic (or higher order) interpolation for finding the interface location are required. In the case where the ghost values are defined by a linear extrapolation, the gradients of the solution converge slowly (at most first order in average) and the convergence rate oscillates, even when the interface location is defined by a quadratic interpolation. The same conclusions hold true for the combination of a quadratic extrapolation for the ghost cells and a linear interpolation. The solution is second-order accurate in all cases. Defining the ghost values with quadratic extrapolations leads to a non-symmetric linear system with a worse conditioning than that of the linear extrapolation case, for which the linear system is symmetric and better conditioned. We conclude that for problems where only the solution matters, the method described in [8] is advantageous since the linear system that needs to be inverted is symmetric. In problems where the solution gradient is needed, such as in Stefan-type problems, higher order extrapolation schemes as described in [6] are desirable.

1 Introduction

The Ghost Fluid Method (GFM), introduced by Fedkiw *et al.* in the context of compressible gas dynamics [4] is an important numerical technique developed to implicitly impose sharp boundary conditions on an irregular interface. In Liu *et al.* [13] the Ghost Fluid Method was used to guide the development of a first-order-accurate symmetric discretization of the variable coefficient Poisson equation in the presence of an irregular domain, where the variable coefficients, the solution and the derivatives of the solution may have jumps across the interface. In Kang *et al.* [11] and Nguyen *et al.* [15], this method was applied to two-phase incompressible flows and to incompressible flame front discontinuities, respectively. A second-order accurate symmetric discretization was developed in Gibou *et al.* [8] for the variable coefficient Poisson equation on irregular domains with Dirichlet boundary conditions instead of jump conditions. This discretization was then extended to fourth-order accuracy in Gibou *et al.* [6]. The discretizations proposed in [13] and in [8] both yield symmetric linear systems that can readily be inverted with a number of fast methods, such as a Preconditioned Conjugate Gradient (PCG) method (see e.g. Golub and Van Loan [9, 16]). This is an advantage over the original level set method for solving the Stefan problem by Chen *et al.* [1] who proposed a non-symmetric scheme. Likewise, a second-order accurate method for the jump condition case was developed in Li *et al.* [12] but with a non-symmetric discretization matrix.

The symmetric discretization presented in [8] has been successfully applied to the simulation of free surface flows in Enright *et al.* [3], multiphase flows with phase-change in Gibou *et al.* [5] and the Stefan Problem in Gibou *et al.* [7]. In this paper, we further analyze the order of accuracy and error distribution of the gradients produced by the method

[*]Computer Science Department, University of California, Santa Barbara, CA 93106.
[†]Computer Science Department, University of California, Santa Barbara, CA 93106.
[‡]Mathematics Department and Research Institute for Basic Sciences, KyungHee University, Seoul, Korea 130-701
[§]Mechanical Engineering Department & Computer Science Department, University of California, Santa Barbara, CA 93106.

of Gibou *et al.* [8, 6]. The goal of this paper is therefore to provide a 'how-to' on the choices one can make when considering the Poisson equation on irregular domains with Dirichlet boundary conditions. Since the same techniques can be applied to diffusion-like as well as Stefan-type problems, this paper can serve as a guide for those problems as well.

In a nutshell, the disadvantage of using a quadratic extrapolation for the ghost value is that the associated linear system is no longer symmetric, as it is the case for [1, 6], and that the condition number of the matrix is significantly larger than that of symmetric discretizations. On the other hand, defining ghost values with quadratic extrapolations (or higher) leads to more accurate computations of the gradients, which in turn impacts the accuracy of moving boundary problems with velocity defined from the solution gradients. Our results are in agreement with the analytical expression for the error in one spatial dimension presented in Jomaa *et al.* [10] for both the linear and quadratic boundary treatments and the observation in McCorquodale *et al.* [14] that a quadratic treatment at the interface leads to second-order accuracy for the solution gradients.

2 Equations and Numerical Methods

2.1 Poisson Equation

Consider a Cartesian computational domain, $\Omega \in R^n$, with exterior boundary, $\partial\Omega$ and a lower dimensional interface Γ that divides the computational domain into disjoint pieces, Ω^- and Ω^+. The variable coefficient Poisson equation is given by

$$\nabla \cdot (\beta(\vec{x})\nabla u(\vec{x})) = f(\vec{x}), \qquad \vec{x} \in \Omega, \tag{1}$$

where $\vec{x} = (x, y, z)$ is the vector of spatial coordinates and $\nabla = (\frac{\partial}{\partial x}, \frac{\partial}{\partial y}, \frac{\partial}{\partial z})$ is the gradient operator. The variable coefficient $\beta(\vec{x})$ is assumed to be continuous on each disjoint subdomain, Ω^- and Ω^+, but may be discontinuous across the interface Γ. $\beta(\vec{x})$ is further assumed to be positive and bounded below by some $\epsilon > 0$. On $\partial\Omega$, either Dirichlet boundary conditions of $u(\vec{x}) = g(\vec{x})$ or Neumann boundary conditions of $u_n(\vec{x}) = h(\vec{x})$ are specified. Here $u_n = \nabla u \cdot \vec{n}$ is the normal derivative of u and $\vec{n}$ is the outward normal to the interface. A Dirichlet boundary condition of $u = u_I$ is imposed on Γ.

In order to separate the different subdomains, we introduce a level set function ϕ defined as the signed distance function:

$$\begin{cases} \phi = -d & \text{for } \vec{x} \in \Omega^-, \\ \phi = +d & \text{for } \vec{x} \in \Omega^+, \\ \phi = 0 & \text{for } \vec{x} \in \Gamma, \end{cases}$$

where d is the distance to the interface. The level set is used to identify the location of the interface as well as the interior and exterior regions.

2.2 Discretization of the Poisson Equation on Irregular Domains

In this section, we recall the discretization of the Poisson equation on irregular domains, as described in Gibou *et al.* [6, 6]. The discretization of the Poisson equation, including the special treatments needed at the interface, is performed in a dimension by dimension fashion. Therefore, without loss of generality, we only describe the discretization in one spatial dimension for the $(\beta u_x)_x$ term. In multiple spatial dimensions, the $(\beta u_y)_y$ and $(\beta u_z)_z$ terms are each independently discretized in the same manner as $(\beta u_x)_x$.

Consider the variable coefficient Poisson equation in one spatial dimension

$$(\beta u_x)_x = f, \tag{2}$$

with Dirichlet boundary conditions of $u = u_I$ on the interface where $\phi = 0$. The computational domain is discretized into cells of size Δx with the grid nodes x_i located at the cell centers. The cell edges are referred to as fluxes so that the two fluxes bounding the grid node x_i are located at $x_{i\pm\frac{1}{2}}$. The solution of the Poisson equation is computed at the grid nodes and is written as $u_i = u(x_i)$. We consider the standard second-order discretization for equation (2) given by

$$\frac{\beta_{i+\frac{1}{2}}(\frac{u_{i+1}-u_i}{\Delta x}) - \beta_{i-\frac{1}{2}}(\frac{u_i-u_{i-1}}{\Delta x})}{\Delta x} = f_i, \tag{3}$$

where $(\beta u)_x$ is discretized at the flux locations.

In order to avoid differentiating the fluxes across the interface where the solution presents a kink, a ghost value is used: Referring to figure 1, let x_I be an interface point between grid points x_i and x_{i+1} with a Dirichlet boundary condition of $u = u_I$ applied at x_I. We define a ghost value u^G_{i+1} at x_{i+1} across the interface, and rewrite equation (3) as

$$\frac{\beta_{i+\frac{1}{2}}(\frac{u^G_{i+1}-u_i}{\Delta x}) - \beta_{i-\frac{1}{2}}(\frac{u_i-u_{i-1}}{\Delta x})}{\Delta x} = f_i. \tag{4}$$

The ghost value u^G_{i+1} is defined by first constructing an interpolant $\tilde{u}(x)$ of $u(x)$ on the left of the interface, such that $\tilde{u}(0) = u_i$, and then defining $u^G_{i+1} = \tilde{u}(\Delta x)$. Figure 1 illustrates the definition of the ghost cells in the case of the linear extrapolation. In this work, we consider linear and quadratic extrapolations defined by:

Linear extrapolation: Take $\tilde{u}(x) = ax + b$ with:

- $\tilde{u}(0) = u_i$,
- $\tilde{u}(\theta\Delta x) = u_I$.

Quadratic extrapolation: Take $\tilde{u}(x) = ax^2 + bx + c$ with:

- $\tilde{u}(-\Delta x) = u_{i-1}$,
- $\tilde{u}(0) = u_i$,
- $\tilde{u}(\theta\Delta x) = u_I$,

where $\theta \in [0, 1]$ refers to the cell fraction occupied by the subdomain Ω^-.

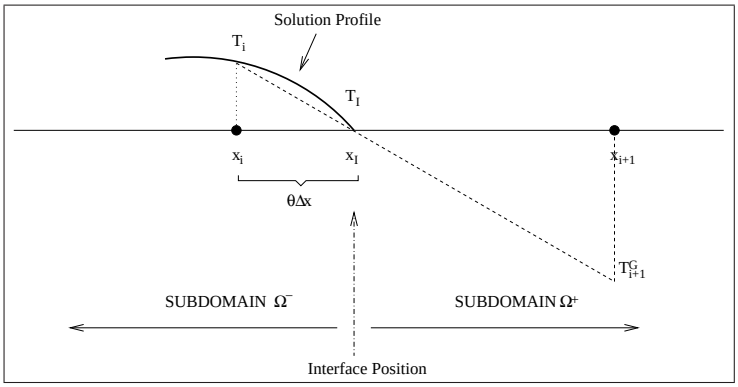

Figure 1: Definition of the ghost cells with linear extrapolation. First, we construct a linear interpolant $\tilde{u}(x) = ax + b$ of u such that $\tilde{u}(0) = u_i$ and $\tilde{u}(\theta\Delta x) = u_I$. Then we define $u^G_{i+1} = \tilde{u}(\Delta x)$.

2.3 Location of the Interface

Referring to figure 1, we compute the location of the interface between x_i and x_{i+1} by finding the zero crossing of the quadratic interpolant $\phi = \phi(x_i) + \phi_x(x_i)x + \frac{1}{2}\phi_{xx}(x_i)x^2$. We note that the quadratic interpolant in ϕ is convex with a positive second order derivative. The location of the interface along the x-direction is calculated as:

$$\theta\Delta x = \begin{cases} \frac{-\phi_x(x_i)+\sqrt{\phi_x^2(x_i)-2\phi_{xx}(x_i)\phi(x_i)}}{\phi_{xx}(x_i)} & \text{if } \phi_{xx}(x_i) > \epsilon \\ -\frac{\phi(x_i)}{\phi_x(x_i)} & \text{if } |\phi_{xx}(x_i)| \leq \epsilon, \end{cases} \tag{5}$$

where ϵ is a small positive number to avoid division by zero. $\phi_x(x_i)$ and $\phi_{xx}(x_i)$ are approximated at x_i using second-order accurate central difference schemes.

2.4 Computation of the Gradients

The solution gradients are computed at each node of the grid: Once we know the location of the interface as described in section 2.3, the Dirichlet boundary value u_I is either given analytically or calculated by quadratic interpolation using neighboring nodal values. Then central-type difference schemes using the value at the interface are used to approximate the component of $\nabla u = (u_x, u_y, u_z)^T$. For example, we define u_x as

$$u_x = \frac{u_I - u_i}{\theta \Delta x} \frac{1}{1+\theta} + \frac{u_i - u_{i-1}}{\Delta x} \frac{\theta}{1+\theta}.$$

We note that in the case where x_{i-1} is outside the domain, we recourse to a first-order formula. Likewise, if θ is too small, we set $u_i = u_I$ to remove the large errors that could occur from dividing by small numbers. In practice we set the threshold to be $\theta = \Delta x$.

Remarks:

- The GFM for the Poisson equation produces second-order accurate solutions even in the case where the interface cuts two adjacent segments (in a least square fit sense).
- The accuracy of the gradient is also second order in the case where the interface and the extrapolation are second-order accurate. Same conclusions are reached in the approach of Chern and Shu [2].

3 Examples

In each example, we consider a domain $\Omega = [-2, 2]^2$ and $\Delta u = f$ on Ω. The level set function ϕ decomposes the domain into separate regions, with $\phi = 0$ defining the interface Γ. The interior region Ω^- is defined by $\phi \leq 0$ while the exterior region Ω^+ is defined by $\phi > 0$. We impose Dirichlet boundary conditions on both the exterior boundary $\partial\Omega$ and the interface Γ. We use the BiCGSTAB algorithm with an incomplete LU preconditioner to solve the linear systems, although one would choose more efficient solvers in practice (for example PCG in the case of symmetric linear systems, GMRES or multigrid methods in the case of non symmetric linear systems). In the examples below, we show the results with different combinations for the definition of the ghost cells and the interpolation to locate the interface. In addition, we present those results in the case where the interface may or may not be smooth, as well as in the case of perturbation of the interface on the grid.

3.1 Numerical Results for a Disk-Shaped Irregular Domain

In this example, the interface Γ is a circle. We use an exact solution of $u(x, y) = e^{\phi}$. We define ϕ as $\phi(x, y) = (x - px)^2 + (y - py)^2 - 1$, where px and py are randomly chosen perturbations. We consider the case with $px = 0$ and $py = 0$ where the circle is centered at the origin, and also the case with $px = 0.691$ and $py = 0.357$ so that the center of the circle does not fall exactly on a grid point. Figure 2 depicts the grids used and the exact solution. The L^∞ errors in the solution and gradient are presented in tables 1 through 8.

3.2 Numerical Results for a Star-Shaped Irregular Domain

In this example, the interface Γ is a star, hence considering the case where the irregular domain has a more complex shape. We use an exact solution of $u(x, y) = \sin(x)\sin(y) + 1$. We define ϕ as $\phi(x, y) = \sqrt{(x - px)^2 + (y - py)^2} - 0.5 - \frac{(y-py)^5 + 5(x-px)^4(y-py) - 10(x-px)^2(y-py)^3}{3((x-px)^2+(y-py)^2)^2}$ for $\sqrt{(x - px)^2 + (y - py)^2} \geq 10^{-4}$ and $\phi(x, y) = -1$ otherwise, where px and py are randomly chosen perturbations. We consider the case with $px = 0$ and $py = 0$ where the star is centered at the origin, and also the case with $px = 0.691$ and $py = 0.357$ so that the center of the star does not fall exactly on a grid point. Figure 3 depicts the grids used and the exact solution. The L^∞ errors in the solution and gradient are presented in tables 9 through 16.

3.3 Numerical Results for a Tilted Square Irregular Domain

In this example, the interface Γ is a tilted square, hence considering the case where the interface has a kink. We use an exact solution of $u(x,y) = e^{-x^2-y^2}$. We define ϕ as $\phi(x,y) = \max[\max(|(\hat{x}-px)-(\hat{y}-py)|-1, |(\hat{y}-py)-(\hat{x}-px)|-1), |(\hat{x}-px)+(\hat{y}-py)|-1]$, where $\hat{x}(x,y) = x\cos(\pi\theta) - y\sin(\pi\theta)$ and $\hat{y}(x,y) = x\sin(\pi\theta) + y\cos(\pi\theta)$. θ, px, and py are randomly chosen perturbations. We consider the case with $\theta = 0.313$, $px = 0$ and $py = 0$ where the tilted square is centered at the origin, and also the case with $\theta = 0.313$, $px = 0.691$ and $py = 0.357$ so that the center of the tilted square does not fall exactly on a grid point. θ is chosen such that the tilted square is not symmetric in the x and y directions. Figure 4 depicts the grids used and the exact solution. The L^∞ errors in the solution and gradient are presented in tables 17 through 24.

3.4 Numerical Results for a Sphere-Shaped Irregular Domain in Three Dimensions

In this example, the interface Γ is defined by a sphere in three dimensions. We use an exact solution of $u(x,y,z) = e^{\phi}$. We define ϕ as $\phi(x,y,z) = (x-px)^2 + (y-py)^2 + (z-pz)^2 - 1$, where px, py and pz are randomly chosen perturbations. We consider the case where the sphere is centered at the $(0,0,0)$, and also the case where the sphere is centered at $(0.249, 0.187, 0.356)$ so that the center of the sphere does not fall exactly on a grid point. The L^∞ errors in the solution and gradient are presented in tables 25 through 32. The highest resolution presented is 256^3 due to memory limitations for the simulation.

4 Synthesis of the Results

In this section, we analyze the order of accuracy and the error distribution of the solution gradients produced by the combination of (1) defining the ghost values with a linear or a quadratic extrapolation and (2) by finding the interface location with a linear or a quadratic interpolant. We also analyze the error distribution and the condition number of the associated linear systems. In all cases, the solution is second-order accurate as demonstrated in [1, 6, 8]. We note that second-order accuracy is the maximum one can reach with the central difference scheme used.

4.1 Accuracy of Gradients

First, we look at the combination of a linear extrapolation for defining the ghost value and a linear interpolation to find the location of the interface. In this case we find that the gradients converge slowly (i.e. at most first order accurate) and their convergence rate oscillate as illustrated in tables 1, 5, 9, 13, 17, 21, 25, and 29. We reach the same conclusion in the case where we use a quadratic interpolation to find the interface location, while still using a linear extrapolation in the definition of the ghost cell value as detailed in tables 2, 6, 10, 14, 18, 22, 26, and 30.

Second, we consider defining the ghost value with a quadratic extrapolation. In this case the gradients are second-order accurate only if the location of the interface is found with an interpolant that is at least quadratic as demonstrated in tables 4, 8, 12, 16, 20, 24, 28, and 32. The accuracy drops to first order at best (in average - also the convergence rates are oscillatory) in the case where the interface location is found with only a linear interpolant as shown in tables 3, 7, 11, 15, 19, 23, 27, and 31.

We conclude that second-order accurate gradients can only be found by defining the ghost cell values with at least a quadratic extrapolation and finding the interface location with at least a quadratic interpolant.

4.2 Distribution of Error for the Solution and its Gradients

In general, the error of the gradient is largest close to the interface regardless of the order of interpolation for the interface location and extrapolation for the ghost values as illustrated in figure 5. Linear extrapolation for the ghost value produces larger errors in the solution close to the interface, while the error in the solution is smooth across all regions for quadratic extrapolation of the ghost value as depicted in figure 6. Defining the ghost values with a linear extrapolation, the gradient converge slowly (at most first-order accurate in average) even if we disregard the large errors contributed by the points within a small band near the interface as demonstrated for the case of the perturbed circle from Ex. 3.1 in tables 33 through 36. This is characteristic of an Elliptic operator, for which errors propagate with infinite speed, and further supports our conclusion that a quadratic extrapolation for the ghost value is required for obtaining second-order accurate gradients.

Effective Resolution	$\|\|u - u_h\|\|_\infty$	Order	$\|\|\nabla u - \nabla u_h\|\|_\infty$	Order
32^2	3.34×10^{-3}	–	9.91×10^{-2}	–
64^2	1.24×10^{-3}	1.43	6.63×10^{-2}	0.58
128^2	3.66×10^{-4}	1.76	5.20×10^{-2}	0.35
256^2	1.03×10^{-4}	1.83	2.90×10^{-2}	0.84
512^2	2.73×10^{-5}	1.92	1.27×10^{-2}	1.19
1024^2	7.11×10^{-6}	1.94	8.10×10^{-3}	0.65

Table 1: Ex.3.1 centered circle. Maximum error for the solution and its gradients in the case where the ghost value is defined by a *linear* extrapolation and the interface location is found with a *linear* interpolant.

Effective Resolution	$\|\|u - u_h\|\|_\infty$	Order	$\|\|\nabla u - \nabla u_h\|\|_\infty$	Order
32^2	6.17×10^{-3}	–	1.99×10^{-1}	–
64^2	2.05×10^{-3}	1.59	1.17×10^{-1}	0.76
128^2	5.68×10^{-4}	1.85	9.92×10^{-2}	0.24
256^2	1.57×10^{-4}	1.85	5.28×10^{-2}	0.91
512^2	4.13×10^{-5}	1.93	2.37×10^{-2}	1.16
1024^2	1.07×10^{-5}	1.95	1.53×10^{-2}	0.63

Table 2: Ex.3.1 centered circle. Maximum error for the solution and its gradients in the case where the ghost value is defined by a *linear* extrapolation and the interface location is found with a *quadratic* interpolant.

4.3 Condition Number and Symmetry of the Linear Systems

Defining the ghost cell value with a linear extrapolation has one advantage over the quadratic extrapolation case: The linear system is symmetric, which allows the use of fast (and straightforward to implement) linear solvers like the preconditioned conjugate gradient [9, 16]. Indeed, the ghost value u_{i+1}^G is given by

$$u_{i+1}^G = \frac{u_I + (\theta - 1)u_i}{\theta} \tag{6}$$

and

$$u_{i+1}^G = \frac{2u_I + (2\theta^2 - 2)u_i + (-\theta^2 + \theta)u_{i-1}}{\theta^2 + \theta} \tag{7}$$

for linear and quadratic extrapolation respectively. Substituting u_{i+1}^G from Eq. (6) into Eq. (4) with $\beta = 1$ yields the symmetric discretization of

$$\frac{\frac{u_I}{\theta} - (1 + \frac{1}{\theta})u_i + u_{i-1}}{(\Delta x)^2} = f_i \tag{8}$$

while substituting Eq. (7) with $\beta = 1$ yields the non-symmetric discretization of

$$\frac{\frac{2u_I}{\theta^2+\theta} - \frac{2}{\theta}u_i + \frac{2}{\theta+1}u_{i-1}}{(\Delta x)^2} = f_i \tag{9}$$

Also, observe that for linear extrapolation, the coefficient of u_i, which corresponds to the diagonal element of the matrix, is increased from 2 to $(1 + \frac{1}{\theta}) > 2$ since $\theta \in [0, 1]$. This increase in the diagonal element is beneficial for iterative methods to converge faster. In the case of a quadratic extrapolation, the diagonal element is increased by a factor of $\frac{1}{\theta}$ but the off-diagonal elements are also increased from 1 to $\frac{2}{\theta+1}$. In both cases the linear systems are diagonally dominant. Defining the ghost values with quadratic extrapolations produces consistently larger condition numbers in the matrices than in the case of a linear extrapolation, as demonstrated in figure 7 for the case of the centered circle from Ex. 3.1. Not surprisingly, the order of interpolation for finding the interface location has a negligible effect on the condition number.

Effective Resolution	$\|\|u - u_h\|\|_\infty$	Order	$\|\|\nabla u - \nabla u_h\|\|_\infty$	Order
32^2	7.59×10^{-3}	–	7.69×10^{-2}	–
64^2	2.12×10^{-3}	1.84	4.51×10^{-2}	0.77
128^2	5.30×10^{-4}	2.00	4.29×10^{-2}	0.07
256^2	1.37×10^{-4}	1.95	2.37×10^{-2}	0.86
512^2	3.42×10^{-5}	2.00	1.09×10^{-2}	1.11
1024^2	8.66×10^{-6}	1.98	6.95×10^{-3}	0.65

Table 3: Ex.3.1 centered circle. Maximum error for the solution and its gradients in the case where the ghost value is defined by a *quadratic* extrapolation and the interface location is found with a *linear* interpolant.

Effective Resolution	$\|\|u - u_h\|\|_\infty$	Order	$\|\|\nabla u - \nabla u_h\|\|_\infty$	Order
32^2	5.43×10^{-3}	–	2.08×10^{-2}	–
64^2	1.44×10^{-3}	1.91	6.46×10^{-3}	1.69
128^2	3.81×10^{-4}	1.92	2.10×10^{-3}	1.62
256^2	9.72×10^{-5}	1.97	5.59×10^{-4}	1.91
512^2	2.46×10^{-5}	1.98	1.30×10^{-4}	2.11
1024^2	6.19×10^{-6}	1.99	3.76×10^{-5}	1.78

Table 4: Ex.3.1 centered circle. Maximum error for the solution and its gradients in the case where the ghost value is defined by a *quadratic* extrapolation and the interface location is found with a *quadratic* interpolant.

Effective Resolution	$\|\|u - u_h\|\|_\infty$	Order	$\|\|\nabla u - \nabla u_h\|\|_\infty$	Order
32^2	5.57×10^{-3}	–	2.46×10^{-1}	–
64^2	1.44×10^{-3}	1.95	1.27×10^{-1}	0.95
128^2	4.34×10^{-4}	1.73	6.39×10^{-2}	0.99
256^2	1.09×10^{-4}	2.00	3.21×10^{-2}	0.99
512^2	2.93×10^{-5}	1.89	1.67×10^{-2}	0.94
1024^2	7.41×10^{-6}	1.99	8.37×10^{-3}	1.00

Table 5: Ex.3.1 perturbed circle. Maximum error for the solution and its gradients in the case where the ghost value is defined by a *linear* extrapolation and the interface location is found with a *linear* interpolant.

Effective Resolution	$\|\|u - u_h\|\|_\infty$	Order	$\|\|\nabla u - \nabla u_h\|\|_\infty$	Order
32^2	9.15×10^{-3}	–	4.98×10^{-1}	–
64^2	2.30×10^{-3}	1.99	2.53×10^{-1}	0.98
128^2	6.63×10^{-4}	1.80	1.23×10^{-1}	1.04
256^2	1.66×10^{-4}	2.00	6.08×10^{-2}	1.02
512^2	4.42×10^{-5}	1.90	3.24×10^{-2}	0.91
1024^2	1.11×10^{-5}	1.99	1.62×10^{-2}	1.00

Table 6: Ex.3.1 perturbed circle. Maximum error for the solution and its gradients in the case where the ghost value is defined by a *linear* extrapolation and the interface location is found with a *quadratic* interpolant.

Effective Resolution	$\|\|u - u_h\|\|_\infty$	Order	$\|\|\nabla u - \nabla u_h\|\|_\infty$	Order
32^2	7.86×10^{-3}	–	1.75×10^{-1}	–
64^2	2.07×10^{-3}	1.92	1.04×10^{-1}	0.75
128^2	5.48×10^{-4}	1.92	5.30×10^{-2}	0.97
256^2	1.38×10^{-4}	1.98	2.69×10^{-2}	0.98
512^2	3.50×10^{-5}	1.99	1.53×10^{-2}	0.81
1024^2	8.79×10^{-6}	1.99	7.70×10^{-3}	0.99

Table 7: Ex.3.1 perturbed circle. Maximum error for the solution and its gradients in the case where the ghost value is defined by a *quadratic* extrapolation and the interface location is found with a *linear* interpolant.

Effective Resolution	$\|\|u - u_h\|\|_\infty$	Order	$\|\|\nabla u - \nabla u_h\|\|_\infty$	Order
32^2	5.19×10^{-3}	–	3.46×10^{-2}	–
64^2	1.45×10^{-3}	1.84	8.92×10^{-3}	1.96
128^2	3.78×10^{-4}	1.94	2.36×10^{-3}	1.92
256^2	9.71×10^{-5}	1.96	6.01×10^{-4}	1.98
512^2	2.46×10^{-5}	1.98	1.50×10^{-4}	2.00
1024^2	6.18×10^{-6}	1.99	3.85×10^{-5}	1.96

Table 8: Ex.3.1 perturbed circle. Maximum error for the solution and its gradients in the case where the ghost value is defined by a *quadratic* extrapolation and the interface location is found with a *quadratic* interpolant.

Effective Resolution	$\|\|u - u_h\|\|_\infty$	Order	$\|\|\nabla u - \nabla u_h\|\|_\infty$	Order
32^2	3.64×10^{-4}	–	1.35×10^{-2}	–
64^2	1.19×10^{-4}	1.61	1.40×10^{-2}	-0.05
128^2	2.54×10^{-5}	2.23	7.54×10^{-3}	0.89
256^2	8.08×10^{-6}	1.65	3.18×10^{-3}	1.25
512^2	2.01×10^{-6}	2.01	1.64×10^{-3}	0.95
1024^2	4.91×10^{-7}	2.03	9.87×10^{-4}	0.73

Table 9: Ex.3.2 centered star. Maximum error for the solution and its gradients in the case where the ghost value is defined by a *linear* extrapolation and the interface location is found with a *linear* interpolant.

Effective Resolution	$\|\|u - u_h\|\|_\infty$	Order	$\|\|\nabla u - \nabla u_h\|\|_\infty$	Order
32^2	4.12×10^{-4}	–	1.59×10^{-2}	–
64^2	1.20×10^{-4}	1.78	1.56×10^{-2}	0.03
128^2	2.67×10^{-5}	2.17	4.78×10^{-3}	1.71
256^2	8.06×10^{-6}	1.73	3.35×10^{-3}	0.51
512^2	2.01×10^{-6}	2.00	1.67×10^{-3}	1.00
1024^2	4.91×10^{-7}	2.03	9.94×10^{-4}	0.75

Table 10: Ex.3.2 centered star. Maximum error for the solution and its gradients in the case where the ghost value is defined by a *linear* extrapolation and the interface location is found with a *quadratic* interpolant.

Effective Resolution	$\|\|u - u_h\|\|_\infty$	Order	$\|\|\nabla u - \nabla u_h\|\|_\infty$	Order
32^2	3.41×10^{-5}	–	1.40×10^{-3}	–
64^2	5.86×10^{-6}	2.54	4.06×10^{-4}	1.79
128^2	9.44×10^{-7}	2.63	5.34×10^{-4}	-0.40
256^2	1.21×10^{-7}	2.97	4.01×10^{-5}	3.74
512^2	1.73×10^{-8}	2.80	1.05×10^{-5}	1.93
1024^2	8.51×10^{-9}	1.02	2.17×10^{-5}	-1.05

Table 11: Ex.3.2 centered star. Maximum error for the solution and its gradients in the case where the ghost value is defined by a *quadratic* extrapolation and the interface location is found with a *linear* interpolant.

Effective Resolution	$\|\|u - u_h\|\|_\infty$	Order	$\|\|\nabla u - \nabla u_h\|\|_\infty$	Order
32^2	3.30×10^{-5}	–	1.46×10^{-3}	–
64^2	6.02×10^{-6}	2.46	4.25×10^{-4}	1.78
128^2	9.55×10^{-7}	2.66	1.13×10^{-4}	1.92
256^2	1.22×10^{-7}	2.97	3.36×10^{-5}	1.74
512^2	1.81×10^{-8}	2.75	8.02×10^{-6}	2.07
1024^2	6.18×10^{-9}	1.55	2.21×10^{-6}	1.86

Table 12: Ex.3.2 centered star. Maximum error for the solution and its gradients in the case where the ghost value is defined by a *quadratic* extrapolation and the interface location is found with a *quadratic* interpolant.

Effective Resolution	$\|\|u - u_h\|\|_\infty$	Order	$\|\|\nabla u - \nabla u_h\|\|_\infty$	Order
32^2	9.73×10^{-4}	–	2.45×10^{-2}	–
64^2	2.53×10^{-4}	1.94	3.95×10^{-2}	-0.69
128^2	6.39×10^{-5}	1.98	2.82×10^{-2}	0.49
256^2	1.74×10^{-5}	1.87	3.01×10^{-2}	-0.10
512^2	4.46×10^{-6}	1.97	7.66×10^{-3}	1.98
1024^2	1.11×10^{-6}	2.00	1.30×10^{-2}	-0.77

Table 13: Ex.3.2 perturbed star. Maximum error for the solution and its gradients in the case where the ghost value is defined by a *linear* extrapolation and the interface location is found with a *linear* interpolant.

Effective Resolution	$\|\|u - u_h\|\|_\infty$	Order	$\|\|\nabla u - \nabla u_h\|\|_\infty$	Order
32^2	1.03×10^{-3}	–	2.81×10^{-2}	–
64^2	2.57×10^{-4}	2.01	3.30×10^{-2}	-0.23
128^2	6.46×10^{-5}	1.99	1.67×10^{-2}	0.98
256^2	1.74×10^{-5}	1.89	7.63×10^{-3}	1.13
512^2	4.47×10^{-6}	1.96	4.46×10^{-3}	0.78
1024^2	1.11×10^{-6}	2.01	2.18×10^{-3}	1.03

Table 14: Ex.3.2 perturbed star. Maximum error for the solution and its gradients in the case where the ghost value is defined by a *linear* extrapolation and the interface location is found with a *quadratic* interpolant.

Effective Resolution	$\|\|u - u_h\|\|_\infty$	Order	$\|\|\nabla u - \nabla u_h\|\|_\infty$	Order
32^2	6.35×10^{-5}	–	2.08×10^{-3}	–
64^2	8.15×10^{-6}	2.96	2.33×10^{-3}	-0.16
128^2	1.29×10^{-6}	2.66	1.13×10^{-3}	1.05
256^2	1.93×10^{-7}	2.74	1.66×10^{-4}	2.76
512^2	5.47×10^{-8}	1.82	1.16×10^{-3}	-2.81
1024^2	2.14×10^{-8}	1.35	1.96×10^{-4}	2.56

Table 15: Ex.3.2 perturbed star. Maximum error for the solution and its gradients in the case where the ghost value is defined by a *quadratic* extrapolation and the interface location is found with a *linear* interpolant.

Effective Resolution	$\|\|u - u_h\|\|_\infty$	Order	$\|\|\nabla u - \nabla u_h\|\|_\infty$	Order
32^2	6.45×10^{-5}	–	2.09×10^{-3}	–
64^2	7.84×10^{-6}	3.04	5.91×10^{-4}	1.82
128^2	1.29×10^{-6}	2.60	1.60×10^{-4}	1.89
256^2	2.02×10^{-7}	2.68	3.92×10^{-5}	2.02
512^2	5.21×10^{-8}	1.96	1.06×10^{-5}	1.89
1024^2	1.82×10^{-8}	1.52	2.70×10^{-6}	1.97

Table 16: Ex.3.2 perturbed star. Maximum error for the solution and its gradients in the case where the ghost value is defined by a *quadratic* extrapolation and the interface location is found with a *quadratic* interpolant.

Effective Resolution	$\|\|u - u_h\|\|_\infty$	Order	$\|\|\nabla u - \nabla u_h\|\|_\infty$	Order
32^2	3.22×10^{-3}	–	1.56×10^{-2}	–
64^2	7.75×10^{-4}	2.06	5.75×10^{-3}	1.44
128^2	1.91×10^{-4}	2.02	2.89×10^{-3}	1.00
256^2	4.71×10^{-5}	2.02	3.30×10^{-4}	3.13
512^2	1.17×10^{-5}	2.01	2.74×10^{-4}	0.27
1024^2	2.93×10^{-6}	2.00	2.34×10^{-2}	-6.42

Table 17: Ex.3.3 centered tilted square. Maximum error for the solution and its gradients in the case where the ghost value is defined by a *linear* extrapolation and the interface location is found with a *linear* interpolant.

Effective Resolution	$\|\|u - u_h\|\|_\infty$	Order	$\|\|\nabla u - \nabla u_h\|\|_\infty$	Order
32^2	3.07×10^{-3}	–	1.20×10^{-2}	–
64^2	7.74×10^{-4}	1.99	8.53×10^{-3}	0.50
128^2	1.94×10^{-4}	2.00	8.78×10^{-3}	-0.04
256^2	4.82×10^{-5}	2.01	2.18×10^{-3}	2.01
512^2	1.21×10^{-5}	1.99	1.91×10^{-3}	0.19
1024^2	2.99×10^{-6}	2.02	2.03×10^{-3}	-0.08

Table 18: Ex.3.3 centered tilted square. Maximum error for the solution and its gradients in the case where the ghost value is defined by a *linear* extrapolation and the interface location is found with a *quadratic* interpolant.

Effective Resolution	$\|\|u - u_h\|\|_\infty$	Order	$\|\|\nabla u - \nabla u_h\|\|_\infty$	Order
32^2	3.15×10^{-3}	–	1.45×10^{-2}	–
64^2	7.75×10^{-4}	2.03	5.75×10^{-3}	1.34
128^2	1.91×10^{-4}	2.02	2.89×10^{-3}	0.99
256^2	4.71×10^{-5}	2.02	3.30×10^{-4}	3.13
512^2	1.17×10^{-5}	2.01	1.35×10^{-4}	1.29
1024^2	2.93×10^{-6}	2.00	2.34×10^{-2}	-7.43

Table 19: Ex.3.3 centered tilted square. Maximum error for the solution and its gradients in the case where the ghost value is defined by a *quadratic* extrapolation and the interface location is found with a *linear* interpolant.

Effective Resolution	$\|\|u - u_h\|\|_\infty$	Order	$\|\|\nabla u - \nabla u_h\|\|_\infty$	Order
32^2	2.74×10^{-3}	–	7.65×10^{-3}	–
64^2	7.15×10^{-4}	1.94	2.14×10^{-3}	1.84
128^2	1.83×10^{-4}	1.97	5.97×10^{-4}	1.84
256^2	4.62×10^{-5}	1.98	1.35×10^{-4}	2.15
512^2	1.16×10^{-5}	1.99	3.79×10^{-5}	1.83
1024^2	2.91×10^{-6}	2.00	8.50×10^{-6}	2.16

Table 20: Ex.3.3 centered tilted square. Maximum error for the solution and its gradients in the case where the ghost value is defined by a *quadratic* extrapolation and the interface location is found with a *quadratic* interpolant.

Effective Resolution	$\|\|u - u_h\|\|_\infty$	Order	$\|\|\nabla u - \nabla u_h\|\|_\infty$	Order
32^2	1.51×10^{-3}	–	7.77×10^{-2}	–
64^2	4.43×10^{-4}	1.77	3.40×10^{0}	-5.45
128^2	7.26×10^{-5}	2.61	4.23×10^{-1}	3.00
256^2	1.99×10^{-5}	1.87	5.24×10^{-2}	3.01
512^2	8.45×10^{-6}	1.23	3.37×10^{-1}	-2.69
1024^2	1.41×10^{-6}	2.59	4.24×10^{-2}	2.99

Table 21: Ex.3.3 perturbed tilted square. Maximum error for the solution and its gradients in the case where the ghost value is defined by a *linear* extrapolation and the interface location is found with a *linear* interpolant.

Effective Resolution	$\|\|u - u_h\|\|_\infty$	Order	$\|\|\nabla u - \nabla u_h\|\|_\infty$	Order
32^2	3.36×10^{-3}	–	1.18×10^{-1}	–
64^2	8.37×10^{-4}	2.01	9.31×10^{-2}	0.34
128^2	2.09×10^{-4}	2.00	3.76×10^{-2}	1.31
256^2	4.98×10^{-5}	2.07	1.85×10^{-2}	1.02
512^2	1.26×10^{-5}	1.98	1.01×10^{-2}	0.88
1024^2	3.22×10^{-6}	1.97	5.02×10^{-3}	1.00

Table 22: Ex.3.3 perturbed tilted square. Maximum error for the solution and its gradients in the case where the ghost value is defined by a *linear* extrapolation and the interface location is found with a *quadratic* interpolant.

Effective Resolution	$\|\|u - u_h\|\|_\infty$	Order	$\|\|\nabla u - \nabla u_h\|\|_\infty$	Order
32^2	1.02×10^{-3}	–	6.10×10^{-2}	–
64^2	2.55×10^{-4}	2.00	3.36×10^{0}	-5.78
128^2	6.04×10^{-5}	2.08	4.19×10^{-1}	3.00
256^2	1.47×10^{-5}	2.04	5.23×10^{-2}	3.00
512^2	3.64×10^{-6}	2.01	3.37×10^{-1}	-2.69
1024^2	9.03×10^{-7}	2.01	4.25×10^{-2}	2.99

Table 23: Ex.3.3 perturbed tilted square. Maximum error for the solution and its gradients in the case where the ghost value is defined by a *quadratic* extrapolation and the interface location is found with a *linear* interpolant.

Effective Resolution	$\|\|u - u_h\|\|_\infty$	Order	$\|\|\nabla u - \nabla u_h\|\|_\infty$	Order
32^2	8.90×10^{-4}	–	1.03×10^{-2}	–
64^2	2.26×10^{-4}	1.98	2.60×10^{-3}	1.99
128^2	5.71×10^{-5}	1.99	6.70×10^{-4}	1.96
256^2	1.43×10^{-5}	1.99	1.69×10^{-4}	1.99
512^2	3.59×10^{-6}	2.00	4.36×10^{-5}	1.96
1024^2	8.96×10^{-7}	2.00	1.07×10^{-5}	2.03

Table 24: Ex.3.3 perturbed tilted square. Maximum error for the solution and its gradients in the case where the ghost value is defined by a *quadratic* extrapolation and the interface location is found with a *quadratic* interpolant.

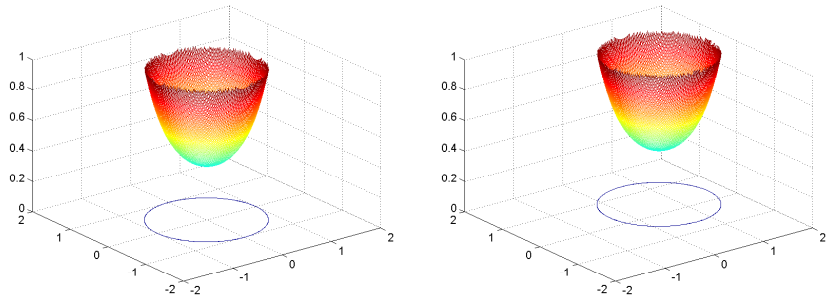

Figure 2: Ex.3.1 grids and exact solution at 256^2 resolution. The figure on the left depicts the case where the circle is centered, while the figure on the right depicts the case where the center of the circle is perturbed.

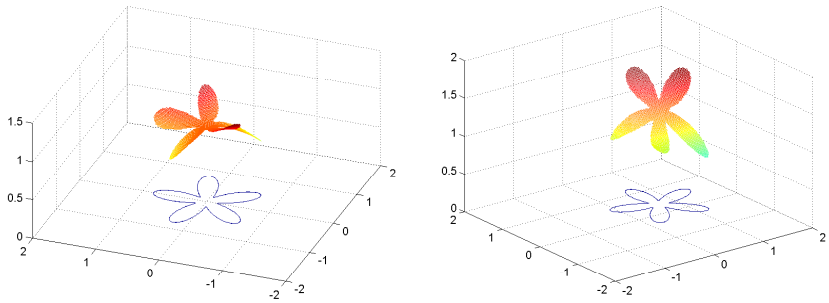

Figure 3: Ex.3.2 grids and exact solution at 256^2 resolution. The figure on the left depicts the case where the star is centered, while the figure on the right depicts the case where the center of the star is perturbed.

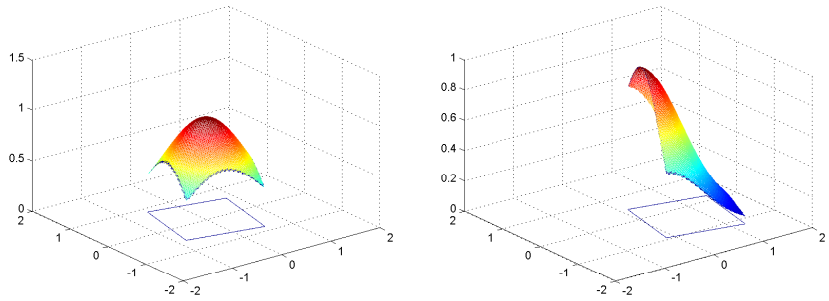

Figure 4: Ex.3.3 grids and exact solution at 256^2 resolution. The figure on the left depicts the case where the tilted square is centered, while the figure on the right depicts the case where the center of the tilted square is perturbed.

Effective Resolution	$\|\|u - u_h\|\|_\infty$	Order	$\|\|\nabla u - \nabla u_h\|\|_\infty$	Order
32^3	7.98×10^{-3}	–	2.01×10^{-1}	–
64^3	1.98×10^{-3}	2.01	1.51×10^{-1}	0.41
128^3	5.05×10^{-4}	1.97	9.36×10^{-2}	0.69
256^3	1.26×10^{-4}	2.01	5.28×10^{-2}	0.83

Table 25: Ex.3.4 centered sphere. Maximum error for the solution and its gradients in the case where the ghost value is defined by a *linear* extrapolation and the interface location is found with a *linear* interpolant.

Effective Resolution	$\|\|u - u_h\|\|_\infty$	Order	$\|\|\nabla u - \nabla u_h\|\|_\infty$	Order
32^3	1.07×10^{-2}	–	2.52×10^{-2}	–
64^3	2.66×10^{-3}	2.01	3.11×10^{-2}	-0.30
128^3	6.66×10^{-4}	2.00	2.44×10^{-2}	0.35
256^3	1.67×10^{-4}	2.00	1.59×10^{-2}	0.62

Table 26: Ex.3.4 centered sphere. Maximum error for the solution and its gradients in the case where the ghost value is defined by a *linear* extrapolation and the interface location is found with a *quadratic* interpolant.

Effective Resolution	$\|\|u - u_h\|\|_\infty$	Order	$\|\|\nabla u - \nabla u_h\|\|_\infty$	Order
32^3	8.02×10^{-3}	–	2.37×10^{-1}	–
64^3	2.05×10^{-3}	1.97	1.63×10^{-1}	0.54
128^3	5.30×10^{-4}	1.95	1.04×10^{-1}	0.64
256^3	1.32×10^{-4}	2.00	5.99×10^{-2}	0.80

Table 27: Ex.3.4 centered sphere. Maximum error for the solution and its gradients in the case where the ghost value is defined by a *quadratic* extrapolation and the interface location is found with a *linear* interpolant.

Effective Resolution	$\|\|u - u_h\|\|_\infty$	Order	$\|\|\nabla u - \nabla u_h\|\|_\infty$	Order
32^3	1.08×10^{-2}	–	2.23×10^{-2}	–
64^3	2.74×10^{-3}	1.97	5.67×10^{-3}	1.98
128^3	6.92×10^{-4}	1.99	1.56×10^{-3}	1.86
256^3	1.74×10^{-4}	1.99	4.10×10^{-4}	1.93

Table 28: Ex.3.4 centered sphere. Maximum error for the solution and its gradients in the case where the ghost value is defined by a *quadratic* extrapolation and the interface location is found with a *quadratic* interpolant.

Effective Resolution	$\|\|u - u_h\|\|_\infty$	Order	$\|\|\nabla u - \nabla u_h\|\|_\infty$	Order
32^3	7.89×10^{-3}	–	2.98×10^{-1}	–
64^3	2.00×10^{-3}	1.98	2.02×10^{-1}	0.56
128^3	5.02×10^{-4}	2.00	1.07×10^{-1}	0.92
256^3	1.26×10^{-4}	2.00	5.51×10^{-2}	0.96

Table 29: Ex.3.4 perturbed sphere. Maximum error for the solution and its gradients in the case where the ghost value is defined by a *linear* extrapolation and the interface location is found with a *linear* interpolant.

Effective Resolution	$\|\|u - u_h\|\|_\infty$	Order	$\|\|\nabla u - \nabla u_h\|\|_\infty$	Order
32^3	1.06×10^{-2}	–	9.39×10^{-2}	–
64^3	2.66×10^{-3}	1.99	1.62×10^{-1}	-0.79
128^3	6.66×10^{-4}	2.00	6.19×10^{-2}	1.39
256^3	1.66×10^{-4}	2.00	2.45×10^{-2}	1.34

Table 30: Ex.3.4 perturbed sphere. Maximum error for the solution and its gradients in the case where the ghost value is defined by a *linear* extrapolation and the interface location is found with a *quadratic* interpolant.

Effective Resolution	$\|\|u - u_h\|\|_\infty$	Order	$\|\|\nabla u - \nabla u_h\|\|_\infty$	Order
32^3	7.97×10^{-3}	–	4.03×10^{-1}	–
64^3	2.08×10^{-3}	1.94	1.81×10^{0}	-2.17
128^3	5.26×10^{-4}	1.98	4.53×10^{-1}	2.00
256^3	1.33×10^{-4}	1.99	3.36×10^{-1}	0.43

Table 31: Ex.3.4 perturbed sphere. Maximum error for the solution and its gradients in the case where the ghost value is defined by a *quadratic* extrapolation and the interface location is found with a *linear* interpolant.

Effective Resolution	$\|\|u - u_h\|\|_\infty$	Order	$\|\|\nabla u - \nabla u_h\|\|_\infty$	Order
32^3	1.07×10^{-2}	–	2.46×10^{-2}	–
64^3	2.74×10^{-3}	1.96	6.70×10^{-3}	1.88
128^3	6.92×10^{-4}	1.99	1.70×10^{-3}	1.98
256^3	1.74×10^{-4}	1.99	4.27×10^{-4}	1.99

Table 32: Ex.3.4 perturbed sphere. Maximum error for the solution and its gradients in the case where the ghost value is defined by a *quadratic* extrapolation and the interface location is found with a *quadratic* interpolant.

Band	Effective Resolution	$\|\|u - u_h\|\|_\infty$	Order	$\|\|\nabla u - \nabla u_h\|\|_\infty$	Order
0	256^2	1.11×10^{-4}	–	3.18×10^{-2}	–
	512^2	2.96×10^{-5}	1.91	1.66×10^{-2}	0.94
	1024^2	7.44×10^{-6}	1.99	8.35×10^{-3}	0.99
	2048^2	1.85×10^{-6}	2.00	4.19×10^{-3}	0.99
5	256^2	1.05×10^{-4}	–	4.70×10^{-4}	–
	512^2	2.68×10^{-5}	1.97	2.29×10^{-4}	1.04
	1024^2	6.91×10^{-6}	1.96	1.27×10^{-4}	0.85
	2048^2	1.69×10^{-6}	2.03	6.63×10^{-5}	0.94
10	256^2	1.05×10^{-4}	–	3.77×10^{-4}	–
	512^2	2.60×10^{-5}	2.01	1.08×10^{-4}	1.80
	1024^2	6.53×10^{-6}	1.99	5.75×10^{-5}	0.91
	2048^2	1.65×10^{-6}	1.98	3.07×10^{-5}	0.90

Table 33: Ex. 3.1 perturbed circle. Maximum error for the solution and its gradients in the case where the ghost value is defined by a *linear* extrapolation and the interface location is found with a *linear* interpolant, when points within a band of 0, 5, and 10 grid cell-width excluded near interface.

Band	Effective Resolution	$\|\|u - u_h\|\|_\infty$	Order	$\|\|\nabla u - \nabla u_h\|\|_\infty$	Order
0	256^2	1.46×10^{-4}	–	1.33×10^{-2}	–
	512^2	3.62×10^{-5}	2.01	6.67×10^{-3}	1.00
	1024^2	9.10×10^{-6}	1.99	3.60×10^{-3}	0.89
	2048^2	2.28×10^{-6}	2.00	1.87×10^{-3}	0.94
5	256^2	1.46×10^{-4}	–	2.95×10^{-4}	–
	512^2	3.62×10^{-5}	2.01	1.09×10^{-4}	1.44
	1024^2	9.10×10^{-6}	1.99	6.25×10^{-5}	0.80
	2048^2	2.28×10^{-6}	2.00	3.32×10^{-5}	0.91
10	256^2	1.46×10^{-4}	–	2.93×10^{-4}	–
	512^2	3.62×10^{-5}	2.01	7.38×10^{-5}	1.99
	1024^2	9.10×10^{-6}	1.99	2.88×10^{-5}	1.36
	2048^2	2.28×10^{-6}	2.00	1.50×10^{-5}	0.94

Table 34: Ex. 3.1 perturbed circle.. Maximum error for the solution and its gradients in the case where the ghost value is defined by a *linear* extrapolation and the interface location is found with a *quadratic* interpolant, when points within a band of 0, 5, and 10 grid cell-width excluded near interface.

Band	Effective Resolution	$\|\|u - u_h\|\|_\infty$	Order	$\|\|\nabla u - \nabla u_h\|\|_\infty$	Order
0	256^2	1.24×10^{-4}	–	2.77×10^{-2}	–
	512^2	3.10×10^{-5}	2.00	1.55×10^{-2}	0.84
	1024^2	7.77×10^{-6}	2.00	7.74×10^{-3}	1.00
	2048^2	1.96×10^{-6}	1.99	3.84×10^{-3}	1.01
5	256^2	1.24×10^{-4}	–	4.04×10^{-4}	–
	512^2	3.10×10^{-5}	2.00	1.58×10^{-4}	1.35
	1024^2	7.77×10^{-6}	2.00	7.29×10^{-5}	1.12
	2048^2	1.96×10^{-6}	1.99	3.55×10^{-5}	1.04
10	256^2	1.24×10^{-4}	–	3.18×10^{-4}	–
	512^2	3.10×10^{-5}	2.00	9.12×10^{-5}	1.80
	1024^2	7.77×10^{-6}	2.00	3.51×10^{-5}	1.38
	2048^2	1.96×10^{-6}	1.99	1.89×10^{-5}	0.90

Table 35: Ex. 3.1 perturbed circle. Maximum error for the solution and its gradients in the case where the ghost value is defined by a *quadratic* extrapolation and the interface location is found with a *linear* interpolant, when points within a band of 0, 5, and 10 grid cell-width excluded near interface.

Band	Effective Resolution	$\|\|u - u_h\|\|_\infty$	Order	$\|\|\nabla u - \nabla u_h\|\|_\infty$	Order
0	256^2	1.65×10^{-4}	–	2.61×10^{-4}	–
	512^2	4.14×10^{-5}	2.00	6.53×10^{-5}	2.00
	1024^2	1.04×10^{-5}	2.00	1.66×10^{-5}	1.98
	2048^2	2.60×10^{-6}	1.99	4.43×10^{-6}	1.91
5	256^2	1.65×10^{-4}	–	2.61×10^{-4}	–
	512^2	4.14×10^{-5}	2.00	6.52×10^{-5}	2.00
	1024^2	1.04×10^{-5}	2.00	1.63×10^{-5}	2.00
	2048^2	2.60×10^{-6}	1.99	4.27×10^{-6}	1.93
10	256^2	1.65×10^{-4}	–	2.61×10^{-4}	–
	512^2	4.14×10^{-5}	2.00	6.52×10^{-5}	2.00
	1024^2	1.04×10^{-5}	2.00	1.63×10^{-5}	2.00
	2048^2	2.60×10^{-6}	1.99	4.27×10^{-6}	1.93

Table 36: Ex. 3.1 perturbed circle. Maximum error for the solution and its gradients in the case where the ghost value is defined by a *quadratic* extrapolation and the interface location is found with a *quadratic* interpolant, when points within a band of 0, 5, and 10 grid cell-width excluded near interface.

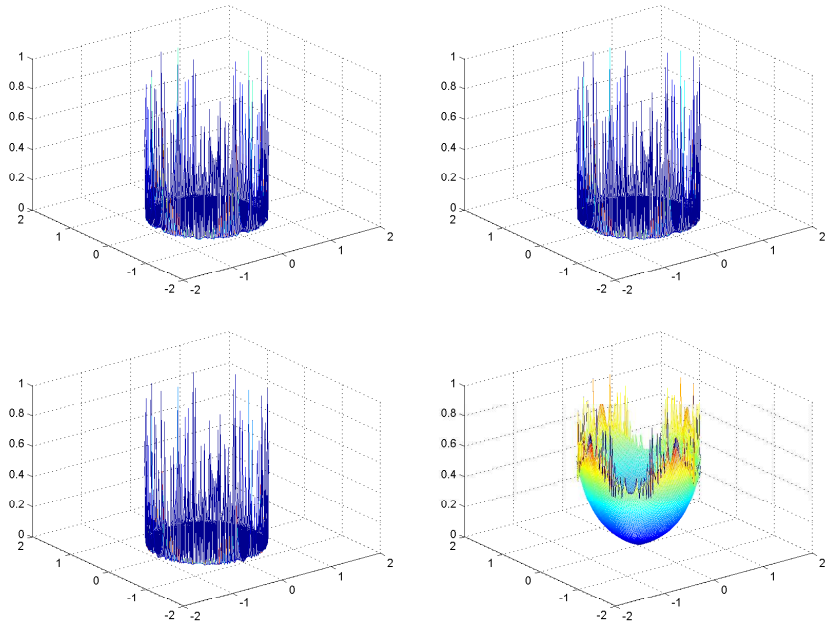

Figure 5: Ex.3.1 centered circle at 256^2 resolution. Normalized error for the gradients of the solution ∇u in the L^∞ norm. The ghost cell values are defined by linear extrapolation of the solution in the top figures and by quadratic extrapolation of the solution in the bottom figures. The interface location is found by linear interpolation ϕ in the left figures and by quadratic interpolation of ϕ in the right figures.

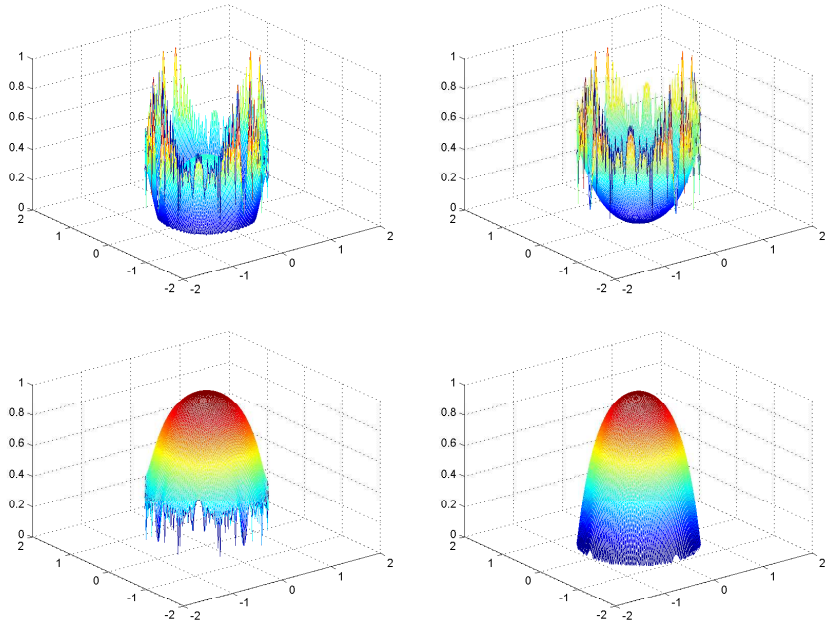

Figure 6: Ex.3.1 centered circle at 256^2 resolution. Normalized error for the solution u in the L^∞ norm. The ghost cell values are defined by linear extrapolation of the solution in the top figures and by quadratic extrapolation of the solution in the bottom figures. The interface location is found by linear interpolation of ϕ in the left figures and by quadratic interpolation of ϕ in the right figures.

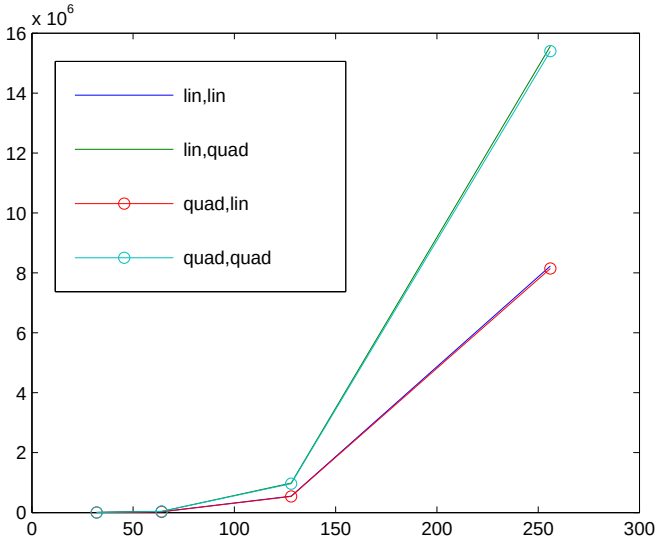

Figure 7: Ex. 3.1 centered circle. Condition numbers versus the grid size. The four curves illustrate the impact of the extrapolation used to define the ghost values and the order of the interpolation for finding the interface location. The two (superimposed) curves with the smallest condition numbers are associated with the linear extrapolation for defining the ghost cells.

5 Acknowledgments

The research of Y.-T. Ng, H. Chen and F. Gibou was supported in part by a Sloan Research Fellowship in Mathematics, by the National Science Foundation under grant agreement DMS 0713858 and by the Department of Energy under grant agreement DE-FG02-08ER15991. The research of C. Min was supported by the Korea Research Foundation Grant funded by the Korean Government (MOEHRD, Basic Research Promotion Fund) (KRF-2008-331-C00045).

6 Conclusions

We have presented numerical evidence for the order of accuracy that can be achieved by the Ghost-Fluid Method for Poisson equations on irregular domains with Dirichlet boundary conditions introduced by Gibou *et al.* [8, 6]. This paper can therefore serve as a guide on how to define ghost values and on how to define the interface location for those interested in the solution of Poisson problems on irregular domains. The same guide can be used for diffusion problems as well as Stefan-type problems. We have shown that a quadratic extrapolation for defining the ghost values and a quadratic interpolation for finding the interface location are necessary to obtain second-order accurate gradients, which in turn may be of interest when considering diffusion dominated moving boundary problems where the interface velocity is defined by the solution gradients. When linear approximation is used for either or both the extrapolation and the interpolation, the gradients converge slowly (at most first-order accurate in average and the convergence rate is oscillatory) across the entire domain, including at locations far away from the interface. In both cases the solution is second-order accurate. We also demonstrated that the symmetric discretization matrix produced by a linear extrapolation for the ghost value is significantly better conditioned relative to the non-symmetric discretization matrix produced by a quadratic extrapolation.

References

[1] S. Chen, B. Merriman, S. Osher, and P. Smereka. A simple level set method for solving Stefan problems. *J. Comput. Phys.*, 135:8–29, 1997.

[2] I.-L. Chern and Y.-C. Shu. A coupling interface method for elliptic interface problems. *J. Comput. Phys.*, 225:2138–2174, 2007.

[3] D. Enright, D. Nguyen, F. Gibou, and R. Fedkiw. Using the particle level set method and a second order accurate pressure boundary condition for free surface flows. In *Proc. 4th ASME-JSME Joint Fluids Eng. Conf.*, number FEDSM2003–45144. ASME, 2003.

[4] R. Fedkiw, T. Aslam, B. Merriman, and S. Osher. A non-oscillatory Eulerian approach to interfaces in multimaterial flows (the ghost fluid method). *J. Comput. Phys.*, 152:457–492, 1999.

[5] F. Gibou, L. Chen, D. Nguyen, and S. Banerjee. A level set based sharp interface method for incompressible flows with phase change. *J. Comput. Phys.*, 222:536–555, 2007.

[6] F. Gibou and R. Fedkiw. A fourth order accurate discretization for the Laplace and heat equations on arbitrary domains, with applications to the Stefan problem. *J. Comput. Phys.*, 202:577–601, 2005.

[7] F. Gibou, R. Fedkiw, R. Caflisch, and S. Osher. A level set approach for the numerical simulation of dendritic growth. *J. Sci. Comput.*, 19:183–199, 2003.

[8] F. Gibou, R. Fedkiw, L.-T. Cheng, and M. Kang. A second–order–accurate symmetric discretization of the Poisson equation on irregular domains. *J. Comput. Phys.*, 176:205–227, 2002.

[9] G. Golub and C. Loan. *Matrix Computations*. The John Hopkins University Press, 1989.

[10] Z. Jomaa and C. Macaskill. The embedded finite difference method for the poisson equation in a domain with and irregular boundary and dirichlet boundary conditions. *J. Comput. Phys.*, 202:488–506, 2005.

[11] M. Kang, R. Fedkiw, and X.-D. Liu. A boundary condition capturing method for multiphase incompressible flow. *J. Sci. Comput.*, 15:323–360, 2000.

[12] R. LeVeque and Z. Li. The immersed interface method for elliptic equations with discontinuous coefficients and singular sources 31:1019–1044, 1994. *SIAM J. Numer. Anal.*, 31:1019–1044, 1994.

[13] X.D. Liu, R. Fedkiw, and M. Kang. A boundary condition capturing method for Poisson's equation on irregular domains. *J. Comput. Phys.*, 154:151, 2000.

[14] P. McCorquodale, P. Colella, D. Grote, and J.-L. Vay. A node-centered local refinement algorithm for Poisson's equation in complex geometries. *J. Comput. Phys.*, 201:34–60, 2004.

[15] D. Nguyen, R. Fedkiw, and M. Kang. A boundary condition capturing method for incompressible flame discontinuities. *J. Comput. Phys.*, 172:71–98, 2001.

[16] Y. Saad. *Iterative methods for sparse linear systems*. PWS Publishing, 1996. New York, NY.